

See discussions, stats, and author profiles for this publication at: <https://www.researchgate.net/publication/49727224>

From Colloidal Stability in Ionic Liquids to Advanced Soft Materials Using Unique Media

ARTICLE *in* LANGMUIR · AUGUST 2011

Impact Factor: 4.46 · DOI: 10.1021/la103942f · Source: PubMed

CITATIONS

60

READS

10

2 AUTHORS:



Kazuhide Ueno
Yamaguchi University
68 PUBLICATIONS 1,204 CITATIONS

[SEE PROFILE](#)



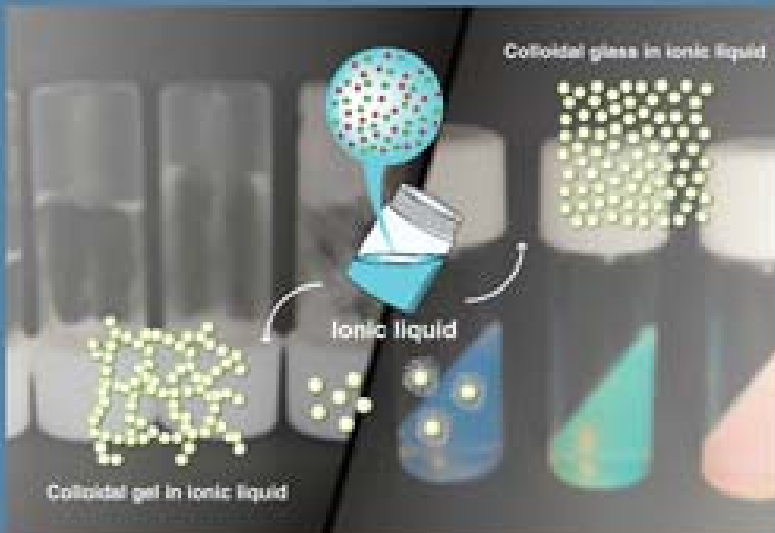
Masayoshi Watanabe
Yokohama National University
348 PUBLICATIONS 14,081 CITATIONS

[SEE PROFILE](#)

Langmuir

The ACS Journal of Surfaces and Colloids

AUGUST 12, 2011
VOLUME 27, NUMBER 16
pubs.acs.org/Longmuir



Soft Materials based on Ionic Liquids and Nanoparticles

(see p. 5A)



ACS Publications
MORE MATERIAL. MORE IDEAS. MORE READ.

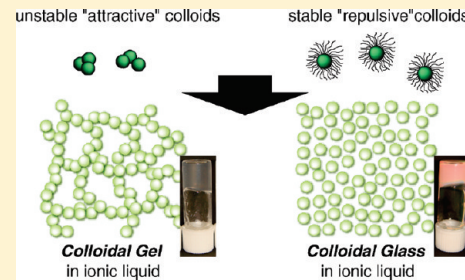
www.acs.org

From Colloidal Stability in Ionic Liquids to Advanced Soft Materials Using Unique Media

Kazuhide Ueno and Masayoshi Watanabe*

Department of Chemistry and Biotechnology, Yokohama National University, 79-5 Tokiwadai Hodogaya-ku, Yokohama 240-8501, Japan

ABSTRACT: Owing to their fascinating properties, ionic liquids (ILs) are now receiving a great deal of attention as alternatives to organic solvents and electrolyte solutions and as synthetic and dispersion media for colloidal systems. Colloidal stability is an essential factor in determining the properties and performance of colloidal systems combined with ILs. The remarkable properties of ILs primarily originate from their highly ionic nature. Although such high ionic strength often causes colloidal aggregation in aqueous and organic suspensions, some colloidal particles can be well suspended in ILs without any stabilizers. In the first part of this article, we focus on recent experiments conducted to investigate the colloidal stability of bare and polymer-grafted silica nanoparticles and on the surface force between silica substrates and ILs. Three different repulsions between colloidal particles (i.e., electrostatic, steric, and solvation forces) are also highlighted, after which a possible interpretation of the results in terms of the stabilization mechanism in ILs both in the presence and in the absence of stabilizers is proposed. The latter part of this article provides an overview of our recent studies on colloidal soft materials with ILs. On the basis of the dispersed states of the silica colloids in ILs, two different soft materials, a colloidal gel and a colloidal glass in ILs, were fabricated. The relationship between their functional properties, such as ionic transport, rheological properties, and optical properties, and the microstructure of the colloidal materials is also described.



1. INTRODUCTION

Ionic liquids (ILs) are composed entirely of ions and liquid with melting points near room temperature (or below 100 °C). In many fields of chemistry and in the chemical industry, ILs are regarded as a “green” alternative to volatile organic solvents used in chemical and catalytic reactions, separations, and purifications.^{1,2} The use of an IL as an electrolyte has also generated considerable interest in the quest for future power sources and electrochemical devices.^{3–5} Such increasing interest in ILs for many applications arises from their unique liquid nature and physicochemical properties, which include (i) a highly concentrated ionic atmosphere that is due to the self-dissociation of ions,⁶ (ii) low vapor pressure and low flammability,⁷ (iii) a wide liquid range with high chemical and thermal stability, (iv) sufficiently high ionic transport, and (v) a structure-forming liquid nature on the nanoscale.^{8,9} Because ILs offer great flexibility in the design of both cationic and anionic structures and their combinations, in principle one can manipulate their properties as desired; therefore, they have been termed “designer solvents.”

ILs have also been exploited as key components of both dispersoids and dispersion media in recent studies. Many researchers have focused on the unique properties of ILs, pursuing novel colloidal systems in ILs such as surfactant solutions,^{10,11} block copolymer micelle solutions,¹² emulsions,^{13,14} and suspensions of solid nanoparticles. Specifically, a number of colloidal systems with ILs have recently been reported with respect to the dispersion of metal and semiconductor nanoparticles. Metal nanoparticle (NP) synthesis in ILs has been most extensively studied using chemical reduction,^{15,16} thermal or photochemical

decomposition,^{17,18} and sputtering or physical vapor deposition.^{19,20} The catalytic metal NPs can be used for a process in organic synthesis with recyclability.^{21,22} Nanostructured inorganic particles have also been prepared using IL as a solvent.²³ The preparation of nanomaterials in ILs and their applications have been reviewed in detail in the literature.^{24–26} Other reports on metal NPs in ILs include the enhancement of colloidal stability in ILs²⁷ and phase transfer to ILs from other dispersed media.²⁸

Interestingly, it has been reported that some colloidal particles can be well suspended in ILs without aggregation, even in the absence of stabilizers such as surfactants and polymers, which are usually employed in stabilization techniques involving aqueous and organic suspensions.^{9,17,22,29,30} Moreover, carbon nanotubes (CNTs) can be dispersed in ILs, forming backy gels,³¹ whereas CNTs tend to form bundles and have low dispersibility in molecular solvents owing to the large cohesive energy density on the basis of the strong $\pi-\pi$ interaction and their very large surface area. In short, IL appears to play a dual role as a dispersion medium and a stabilizer that prevents particle agglomeration. Although a few plausible interpretations have been made in previous studies, recent research has been focused on clarifying the anomalous stabilization mechanism of colloidal particles in ILs. It is important to have a thorough understanding of colloidal stabilization to facilitate their application in many colloid–IL systems. In the first part of this article, we highlight the colloidal

Received: October 1, 2010

Revised: December 10, 2010

Published: January 04, 2011

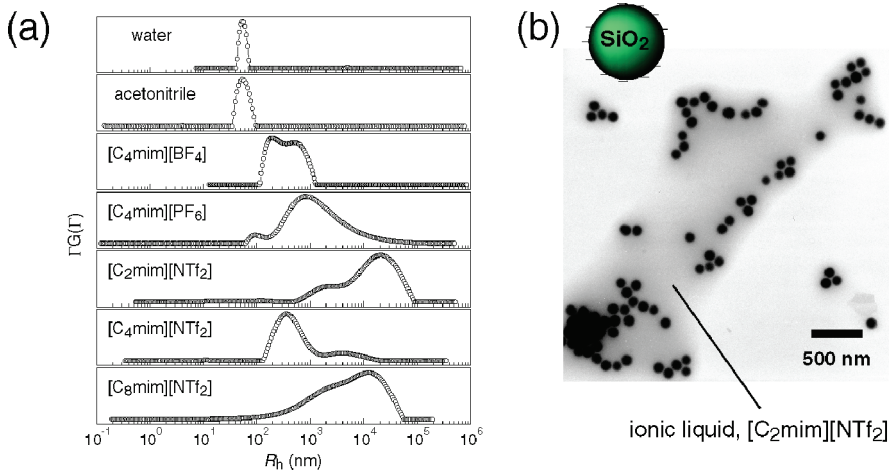


Figure 1. (a) Size distribution curves for the bare silica particles in deionized water, acetonitrile, and ILs measured by DLS. $[C_n\text{mim}]$ stands for 1-alkyl-3-methylimidazolium, and $[\text{NTf}_2^-]$ stands for bis(trifluoromethane sulfonyl)amide. (b) TEM image of a dilute dispersion of bare silica particles in $[C_2\text{mim}][\text{NTf}_2]$. The black spots correspond to the silica particles, and the gray portion shows the image of $[C_2\text{mim}][\text{NTf}_2]$. Reproduced from ref 38.

stability of solid particles suspended in ILs and provide possible interpretations of their stabilization mechanism. Three different repulsions between colloidal particles (i.e., electrostatic, solvation (structural), and steric forces) are discussed in this article.

Among the different attempts to utilize colloid–IL systems, the fabrication of functional materials has been an attractive topic. The combination of ILs and functional nanoparticles and the self-assembled structure of colloidal particles in ILs allows the fabrication of novel nanohybrid materials.^{32,33} Because the addition of colloidal materials to fluids occasionally provides soft solid material above certain particle concentrations, this procedure can be used to fabricate IL-based solid electrolytes.^{34–36} The colloidal soft materials of ILs are of interest because they can be readily prepared and their inherent yielding or flow behavior allows easy processing under applied stress. In the latter part of this article, we present functional soft materials consisting of colloid–IL systems with a variety of different functional properties. In particular, we deal with two categories of soft solid materials consisting of colloidal particles and ILs—a colloidal gel and a colloidal glass—and highlight their functional properties. Moreover, we demonstrate the transition from colloidal glass to gel in ILs with thermosensitive polymer-grafted silica nanoparticles.

2. COLLOIDAL STABILITY IN ILS

Colloidal particles are kinetically stabilized by mutual repulsions between particles, namely, electrostatic, steric, and solvation (structural) forces in typical suspensions. If these particles are not stabilized, they form aggregates owing to interparticle van der Waals attraction.³⁷ Here, we focus on the effect of these three different types of repulsions on the colloidal stability in ILs in the absence and the presence of stabilizers other than the IL medium.

2-1. Electrostatic Stabilization. The electrostatic force is a common, well-studied repulsion used to stabilize colloidal particles in aqueous and organic media. Ionic groups on colloidal surfaces dissociate their counterions in the vicinity of the surface and form an electrical double layer (EDL), which induces electrostatic repulsion between particles. Electrostatic repulsion is based on the classical Debye–Hückel theory, which is applicable to dilute systems. For the sake of simplicity, we previously adopted the classical theory of electrostatic interaction between

colloidal particles in ILs for the first approximation, and the theory implied that the electrostatic repulsive force hardly stabilizes charged silica particles in the ILs because of the high ionic concentration of the ILs ($>1.5 \text{ mol L}^{-1}$).³⁸

Although the examined theory simply assumed the ILs to be an unstructured, continuous liquid, the structure of EDL in ILs has been the subject of debate because of the highly charge-concentrated nature of ILs in which no solvents exist.³⁹ The extended Gouy–Chapman theory, which considers the ion size of ILs, has been applied to calculate the thickness of the EDL.⁴⁰ However, it was still less than the molecular size of the ILs, thus the electrostatic repulsion may be considerably weakened in ILs, especially in cases of long interparticle distances. Moreover, recent computer simulation studies revealed charge-density oscillations in the EDL of ILs confined between charged solid surfaces.^{41,42} This interesting oscillation profile in the vicinity of the IL–solid interface is probably due to another source of repulsion, such as solvation and structural forces, rather than electrostatic repulsion (vide infra).

The colloidal stability of the negatively charged, bare silica particles was also experimentally evaluated in the ILs.³⁸ Dynamic light scattering (DLS) results and the transmission electron microscope (TEM) image of the monodispersed silica colloidal dispersion (62 nm in mean radius) are shown in Figure 1a,b, respectively. It should be noted that ILs can be observed by a scanning electron microscope (SEM) or a TEM without evaporation and accumulation of electronic charges, despite the high vacuum conditions and electron beam irradiation. All of the results shown in Figure 1 indicate that charged silica nanoparticles are not electrostatically stable in the ILs. Hence, the electrostatic charge stabilization appears to be insufficient owing to the high ionic strength of the ILs and the resulting surface-charge screening.

2-2. Solvation Force in ILs. Another possible repulsion we discuss here is the solvation (structural) force. When liquid molecules are confined between two flat surfaces on the nanometer scale, ordered or layered structures resulting in a liquid density oscillation are often formed in the vicinity of a solid–liquid boundary. The repulsive solvation force originates by escaping the disruption of the ordering/layering structures on approach. The oscillatory solvation force has been extensively studied

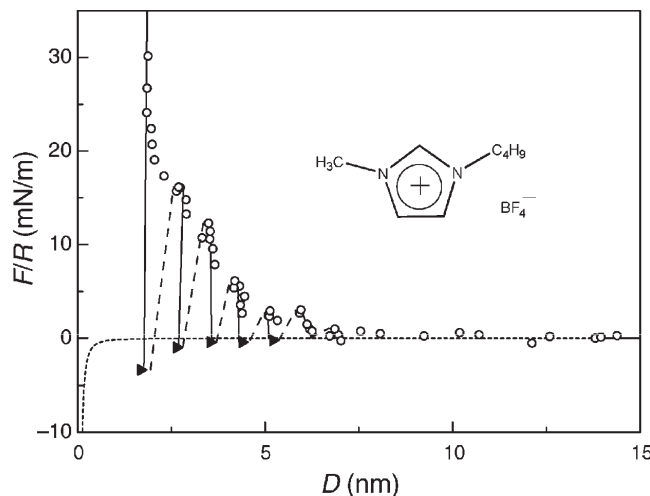


Figure 2. Normal force scaled with the surface radius of curvature (F/R) as a function of the surface separation D between silica surfaces in $[C_4\text{mim}][\text{BF}_4]$. The open circles (○) show data on approach, whereas the solid triangles (▲) show data on retraction with D calculated from measured stable jump-out positions and spring constants divided by the radius of the surface curvature (k/R). The dotted lines represent van der Waals attractions calculated from Lifshitz's theory assuming that the ILs are a continuous medium with a Hamaker constant of 8.9×10^{-22} J for $[C_4\text{mim}][\text{BF}_4]$. The solid and dashed lines indicate stable and unstable regions, respectively, in force profiles. Reproduced from ref 51.

and identified in many molecular liquids, including octamethylcyclotetrasiloxane,⁴³ liquid crystals,⁴⁴ and aqueous solutions,⁴⁵ by surface force measurement. Recently, the surface force in ILs was measured using an atomic force microscope (AFM)⁴⁶ and a surface force apparatus (SFA).^{47–49} Systematic surface force studies conducted by Atkin et al. confirmed the well-defined oscillating solvation force in aprotic and protic ILs on various surfaces.⁵⁰ These results are consistent with the results obtained from a computer simulation, which show an oscillatory profile of density and an electrostatic potential for a model IL confined between flat charged surfaces.^{41,42} As an example, Figure 2 shows our result on the surface force between silica surfaces in an aprotic IL, $[C_4\text{mim}][\text{BF}_4]$.⁵¹ Upon approach, the repulsive force with periodic jump-in was detected. The resulting force profile appeared to be oscillating rather than monotonic, with an oscillation periodicity of 0.7 to 0.8 nm. These oscillations were in agreement with the calculated dimensions of ion pairs for the IL (0.68 nm), which was the cubic root of the molecular volume calculated from the known density and the molecular weight. The observed oscillating surface forces and MD simulation indicate that the ion pairs are arranged in a layer-by-layer structure in the vicinity of solid surfaces.

Unlike typical molecular liquids, the layered structure of ILs can be formed even in the absence of the confinement effect because ions of ILs should strongly interact with a single-sided charged surface. Furthermore, the intrinsic structure-forming properties of ILs in the bulk^{8,9} could facilitate the formation of a remarkably well defined layered structure at charged surfaces. High-energy X-ray reflectivity measurements revealed a strong molecular layering of aprotic ILs on negatively charged, single-sided sapphire (001) surfaces.⁵²

2-3. Possible Stabilization in the Absence of Stabilizers.

Figure 3 shows possible stabilization mechanisms of colloidal particles without stabilizers in ILs. For the IL-based steric

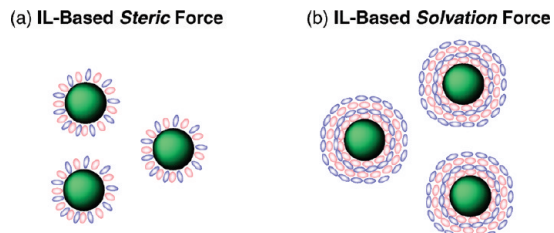


Figure 3. Schematic illustration of colloidal stabilization in ILs without stabilizers: (a) the ionic-liquid-based steric force and (b) the ionic-liquid-based solvation force.

stabilization (Figure 3a), IL molecules (ions) that strongly attached to colloidal surfaces may be bulky enough to separate each colloidal surface in certain cases. Ott et al. reported that the formation of *N*-heterocyclic carbens derived from imidazolium cations on Ir(0) nanoparticles contributed to the steric stabilization of nanoparticles in imidazolium ILs.⁵³ Many ILs, especially cations, are composed of both nonpolar alkyl groups and polar ionic groups, which can be adsorbed onto either hydrophilic or hydrophobic surfaces as seen in common surfactants. Hence, the amphiphilic property may be relevant to the enhanced colloidal stability in ILs. It was recently reported that Ru nanoparticles were surrounded by the nonpolar alkyl chains of the cation in the structured IL, $[C_4\text{mim}][\text{NTf}_2]$.⁵⁴ In this case, the nonpolar alkyl chains appeared to work as a protective group that prevents aggregation. Lu and Dyson reported the remarkable anion effect on gold nanostructures and microstructures fabricated in ILs.⁵⁵ There is a possibility that the affinity of the anions for the gold surface also influences the stability of gold clusters related to the resulting gold nanostructures and microstructures. Thus, IL-based steric stabilization would be optimized by the appropriate choice of ions of ILs and/or surface modification considering such affinity between the ions and colloidal surfaces.

For the IL-based solvation force (Figure 3b), the multilayered structure of ILs can reach several nanometers (e.g., Figure 2), which leads to the solvation force inducing longer-range repulsion as compared to the IL-based steric force. Smith et al. recently reported the long-term stability of charged silica particles in a protic IL, ethylammonium nitrate (EAN), and the solvation force was found to be responsible for this surprising stabilization.⁵⁶ They also reported that the suspensions become unstable in the presence of a small amount of water, and the destabilization was again evidenced by the decreased solvation force upon the addition of water. We also observed that smaller silica nanoparticles (6 nm in radius) were well suspended in $[C_4\text{mim}][\text{BF}_4]$ (probably by the IL-based solvation force),⁵⁷ even though the larger charged silica nanoparticles were unstable in a series of aprotic ILs (Figure 1). This might be derived from the effect of particle size because the van der Waals attraction between particles increases with increasing particle size.³⁷ For larger particles, the energy linked to the thermal motion of the particles may be high enough to overcome the repulsive barrier, leading to aggregation. The strength of the solvation force depends on factors such as the ionic structure of ILs, surface charge density, surface chemistry and roughness, and amount of water.^{50,56} However, it is important to note that IL-based solvation stabilization must also be a plausible explanation for the reported unusual colloidal stability in ILs.

2-4. Steric Stabilization by Polymer Grafting. Surfactants and polymers have often been employed to stabilize colloids via

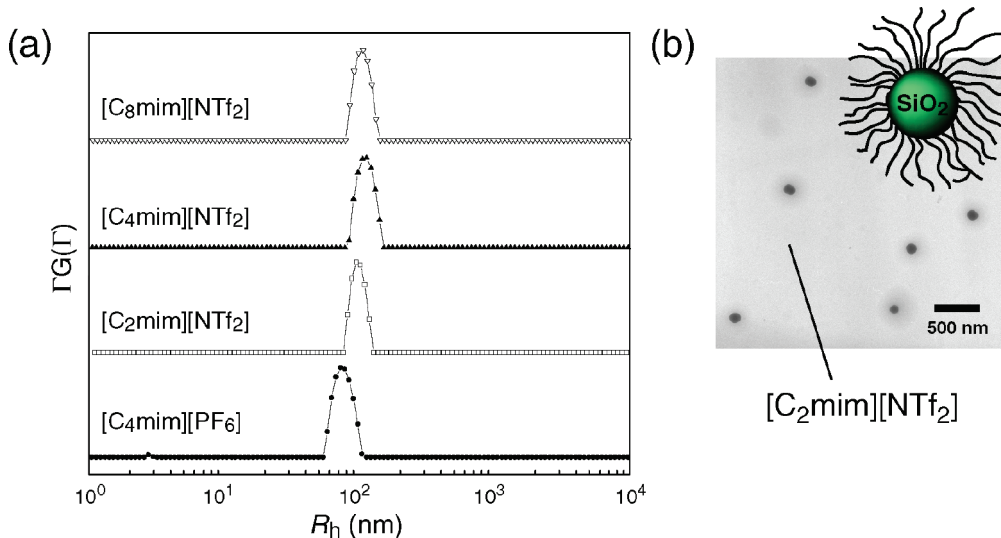


Figure 4. (a) Size distribution curves for PMMA-grafted silica particles (hydrodynamic radius of 107 nm) in ILs measured by DLS. (b) TEM image of a dilute dispersion of PMMA-grafted silica particles in $[C_2\text{mim}][\text{NTf}_2]$. Reproduced from ref 38.

interparticle steric hindrance. In contrast to electrostatic stabilization, the adsorption and grafting of a polymer onto a colloid surface leads to either steric stabilization or the bridging flocculation of the particles. The low surface concentration and high molecular weight of the grafted polymer increase the possibility of interparticle bridging by the polymers. Therefore, we prepared poly(methyl methacrylate)(PMMA)-grafted silica nanoparticles (PMMA-g-NPs) by surface-initiated atom-transfer radical polymerization, which results in a high graft density and high controllability of the molecular weight.³⁸ Particles that consisted of a silica core with a mean radius of 61 nm and grafted PMMA with an average molecular weight of 53 000 g/mol and a graft density of 0.21 chains nm^{-2} were used for subsequent experiments.

The colloidal stability of sterically stabilized particles also depends on the solubility of the grafted polymer in the dispersion medium. In a good solvent, particles have a strong repulsive force owing to the excluded volume effect, which prevents interpolymer penetration of the PMMA-grafted silica nanoparticles. Conversely, in a poor solvent, the attraction becomes dominant because of the insolubility of the grafted PMMA. Among the ILs examined in this study, PMMA is soluble in $[C_4\text{mim}][\text{PF}_6]$ and $[C_n\text{mim}][\text{NTf}_2]$, whereas it is insoluble in $[C_4\text{mim}][\text{BF}_4]$. As expected, the colloidal stability was clearly dependent on the solubility of PMMA in the ILs. In the $[C_4\text{mim}][\text{BF}_4]$ dispersion, PMMA-g-NPs were phase-separated, even during sample preparation, indicating the aggregation of PMMA-g-NPs in the IL. However, a narrow size distribution was observed for the dispersions in $[C_n\text{mim}][\text{NTf}_2]$ and $[C_4\text{mim}][\text{PF}_6]$, as seen in Figure 4a. The TEM image also showed excellent dispersibility of the PMMA-grafted silica particles in the $[C_2\text{mim}][\text{NTf}_2]$ dispersion (Figure 4b, see also Figure 9c for concentrated suspensions). Thus, steric hindrance by additional stabilizers is applicable to the stabilization of colloidal particles in ILs, as seen in typical colloidal suspensions.

3. SOFT MATERIALS BASED ON COLLOIDAL PARTICLES AND ILs

Owing to interesting colloidal phenomena, including reinforcement, shear thinning, shear thickening, gelation, and the

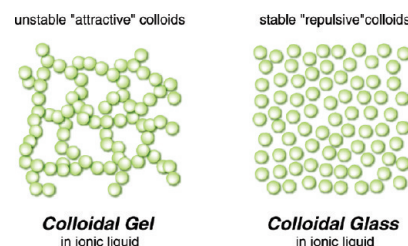


Figure 5. Schematic illustration of the colloidal soft material in ILs: colloidal gel and colloidal glass.

shear-induced sol–gel phase transition, colloidal soft materials have played an important role as major components in a wide variety of well-established applications. There are two categories of solidlike amorphous soft materials that are composed of colloidal particles, a colloidal gel, and a colloidal glass.⁵⁸ In the colloidal gel, the dispersion of colloidal particles is unstable in the dispersion medium and the particles form interconnecting 3D networks that percolate through the entire volume of the suspension medium. Colloidal glass is typically formed in highly concentrated suspensions in which the colloidal particles are trapped within cages formed by the nearest particle neighbors. Colloidal glass has solidlike properties owing to cage effects. Both of these soft materials can be prepared with ILs. Such materials have the potential for use as solid electrolytes for electrochemical devices. Here, we describe two different soft materials produced using ILs, the colloidal gel and the colloidal glass in ILs, on the basis of the colloidal stability of particles on the ILs (Figure 5).

3-1. Colloidal Gel in ILs. The colloidal gel was prepared from unstable silica nanoparticles in ILs.⁵⁹ When fumed silica nanoparticles with a diameter of 12 nm were used, gelation could be achieved by the addition of only a few weight percent of the silica nanoparticles (Figure 6a). Owing to poor colloidal stability, the silica nanoparticles formed interconnecting aggregates with a loosely outspread fractal structure in $[C_2\text{mim}][\text{NTf}_2]$, as seen in the TEM image (Figure 6b). Gelation with even a small number of silica nanoparticles was a consequence of the formation of this network structure. The particle concentration required for the

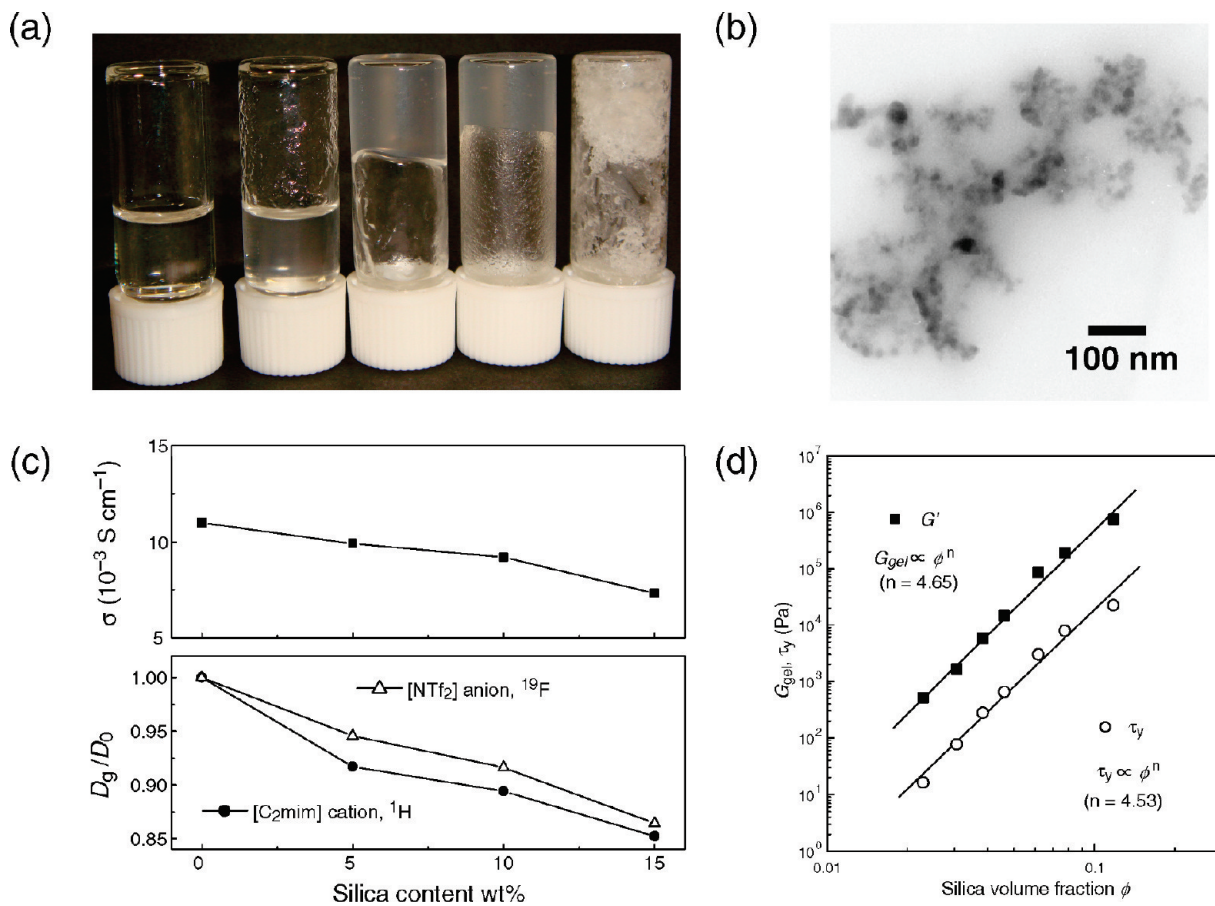


Figure 6. Colloidal gel consisting of silica nanoparticles (6 nm in average radius) and $[\text{C}_2\text{mim}][\text{NTf}_2]$. (a) Photographs of the binary mixtures depending on silica nanoparticle concentrations. The silica nanoparticle concentrations were 0, 1, 3, 5, and 15 wt % from left to right. (b) TEM image of a 5 wt % colloidal gel. The focus could not be sharpened because of the presence of an IL. (c) Concentration dependence of ionic transport properties at 30 °C: ionic conductivity (σ) and relative ionic self-diffusion coefficient (D_g/D_0). (d) Mechanical properties at 25 °C obtained by rheological measurement: gel modulus (G_{gel}) and yield stress (τ_y) as a function of the volume fraction of silica nanoparticles. Reproduced from ref 59.

colloidal gelation depended on the size of the particles, with 40 wt % silica particles being required for gelation in the case of larger silica nanoparticles (300 nm in diameter). For colloidal gels formed by space-spanning particle aggregates, the critical volume fraction for gelation (ϕ_c) was theoretically predicted to be⁶⁰

$$\phi_c \approx \left(\frac{4\pi \Delta \rho g R^4}{3kT} \right)^{(3 - d_f)/(1 + d_f)}$$

where $\Delta \rho$ is the difference between the density of particles and that of the suspending fluid, g is the acceleration of gravity, R is the particle radius, k is the Boltzmann constant, T is the absolute temperature, and d_f is the fractal dimension of the aggregated structure. Thereafter, the ionic transport and mechanical properties were evaluated for colloidal gels composed of small silica particles (12 nm in diameter).

Figure 6c,d shows the ionic transport and mechanical properties, respectively, of colloidal gels with different silica concentrations. The addition of silica particles had little impact on the ionic conductivity. The conductivity of the colloidal gel reached a value of ca. $10^{-2} \text{ S cm}^{-1}$ at 30 °C, which is comparable to that of pure $[\text{C}_2\text{mim}][\text{NTf}_2]$. Only a 30% decrease in conductivity was observed in response to the addition of 15 wt % silica nanoparticles, and the appearance of this colloidal gel became powderlike

under these conditions. The relative diffusivity of the ions is given by D_g/D_0 where D_0 and D_g are the self-diffusion coefficients of the diffusive species measured by PGSE-NMR in the neat IL and in the colloidal gels, respectively. The relative diffusivity of the ions decreased slightly as the silica concentration increased, primarily because of the obstruction of the silica particles. The reduction in D_g/D_0 for the $[\text{C}_2\text{mim}]$ cation was larger than that for the $[\text{NTf}_2]$ anion in the colloidal gel, indicating that the diffusion of the cations was more restricted by their preferential interaction with the negatively charged silica surface. These findings do not conflict with those of previous studies conducted to evaluate the IL–silica interface using other techniques such as surface force measurement⁴⁶ and sum-frequency vibrational spectroscopy;⁶¹ therefore, they demonstrate the presence of cations of ILs in proximity to the surface.

In contrast to the small change in ionic transport properties, the mechanical properties, gel modulus (G_{gel}), and yield stress (τ_y) increased drastically with increasing concentration of silica nanoparticles. The mechanical properties exhibit a power-law dependence on the volume fraction (ϕ) of particles; $G' \propto \phi^n$, $n = 4.65$ for G_{gel} , and $n = 4.53$ for τ_y . Thus, we could control the mechanical properties over more than 3 orders of magnitude by adjusting the number of silica particles whereas the inherent properties of ILs other than the mechanical properties were nearly maintained in the colloidal gels. The enhancement of the

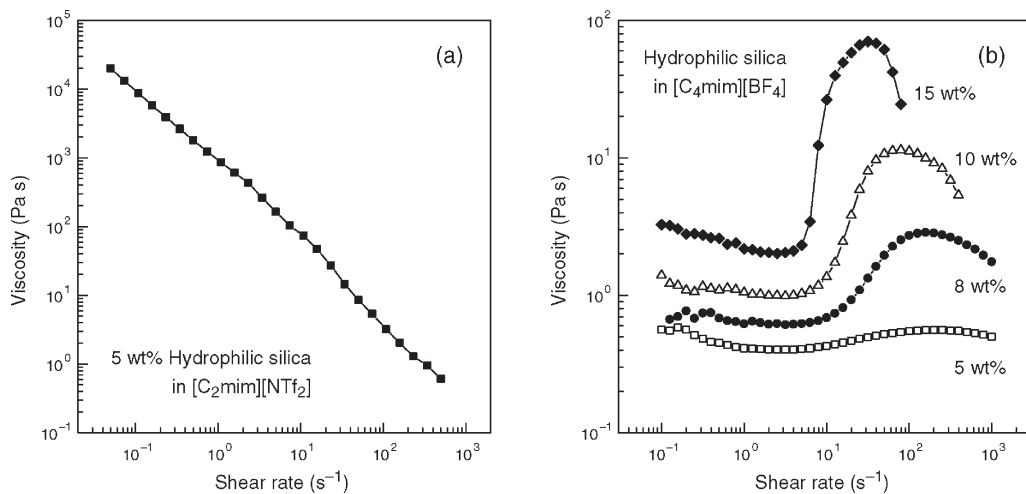


Figure 7. Shear rate dependence of viscosity for (a) a colloidal gel composed of 5 wt % hydrophilic silica nanoparticles (average radius of 6 nm) and $[C_2\text{mim}][\text{NTf}_2]$ and (b) stable suspensions of hydrophilic silica nanoparticles in $[C_4\text{mim}][\text{BF}_4]$ with different silica particle concentrations. Reproduced from ref 57.

mechanical properties was attributed to the particulate network. Unlike chemically cross-linked gels, silica particle gels are loosely bound to each other; therefore, the network can be disrupted by sufficient shear application. As a result, the colloidal gel shows fluidity under shear (the shear-thinning effect) but can be solidified again by removing the shear.

Silica-based colloidal gels can be macroscopically characterized as phase-separated binary systems in which ionic transport is mostly free from interaction with the silica surface and is affected only by the obstruction of the interconnecting silica network. A large open-network structure derived from the lower silica concentrations minimizes the obstruction of ionic migration. The reduction in the total ionic carrier concentration remains minimal owing to the low concentration of silica particles. Consequently, the remarkably high conductivity is due to both the high mobility and the carrier concentration in the system, whereas the particulate network lends largely improved mechanical properties.

The ionic structure of ILs and the surface chemistry of colloids affect the formation of colloidal gels.⁵⁷ Indeed, no colloidal gelation was observed in certain ILs (e.g., BF_4 -based ILs and ILs containing a hydroxyl group) with hydrophilic, unmodified fumed silica. As compared to the colloidal gel of $[C_2\text{mim}][\text{NTf}_2]$, which showed a decrease in shear viscosity in response to shear (shear-thinning behavior, Figure 7a), these suspensions displayed low viscosity at a low shear rate. These findings are characteristic of a stable suspension. In such systems, the silica particles may be stabilized by the IL-based steric and/or the IL-based solvation force. Furthermore, these stable suspensions exhibited an interesting rheological property; specifically, a sudden increase in shear viscosity (shear thickening behavior, Figure 7b) was detected in response to a high shear rate. A variety of different rheological responses of colloidal suspensions possessing the unique properties of ILs may allow the application of a functional rheological fluid. Colloidal gelation occurred in response to the addition of hydrophobic methyl-substituted fumed silica in many ILs that are BF_4 -based or contain a hydroxyl group. Although surface modification frequently improves the colloidal stability by steric hindrance as mentioned in the previous section, the methyl-substituted surface of the hydrophobic silica has

a poor affinity for the examined ILs and repulsive interaction is absent between the hydrophobic particles.⁵⁷ Accordingly, the methyl-substituted silica nanoparticles appear to be more suitable for obtaining colloidal gels from ILs.

3-2. Colloidal Glass in ILs. To prepare another colloidal soft material, namely, colloidal glass in ILs, we used monodisperse, sterically stabilized PMMA-g-NPs in $[C_2\text{mim}][\text{NTf}_2]$.^{62,63} Figure 8a shows the colloidal suspensions of different concentrations of PMMA-g-NPs in IL. At lower particle concentrations, PMMA-g-NPs were well suspended in the IL without any aggregation or sedimentation, and the dilute suspensions showed liquidlike behavior (samples B and C). However, the suspensions (samples D–F) became solidified (i.e., underwent a colloidal glass transition) above a certain particle concentration and exhibited different colors depending on the particle concentration. It is well known that the colloidal glass transition occurs at a particle volume fraction (ϕ) of 0.58 for hard-sphere particles.⁶⁴ We investigated the critical glass-transition volume fraction (ϕ_g) for these PMMA-g-NPs in the IL as a function of the effective volume fraction (ϕ_{eff}) that takes into consideration the grafted PMMA chains swollen by the IL. Through systematic rheological measurements, the ϕ_g value for PMMA-g-NPs was found to be $\phi_{\text{eff}} = 0.70–0.74$,⁶³ which is higher than that for hard-sphere systems because of the soft interparticle interaction of PMMA-g-particles. Concentrated suspensions with values greater than ϕ_g exhibited a storage modulus (G') that was evidently higher than the loss modulus (G'') upon dynamic rheological measurement, indicating a typical soft, solidlike response (Figure 8b). As compared to the colloidal gel in ILs, higher particle concentrations were necessary for this type of soft material to be formed. With respect to rheological properties, the colloidal glass also exhibited shear-thinning behavior and a power-law dependence of an elastic modulus plateau on ϕ_{eff} that was analogous to that of the colloidal gels.⁶³

In a manner similar to that for the colloidal gels, the ionic transport properties were studied to evaluate potential applications in soft-solid electrolytes. Figure 8c,d shows ionic conductivity and ionic diffusion behavior, respectively, in colloidal glass with different particle concentrations. For the ionic conductivity, the onset volume fraction at which the conductivity started to

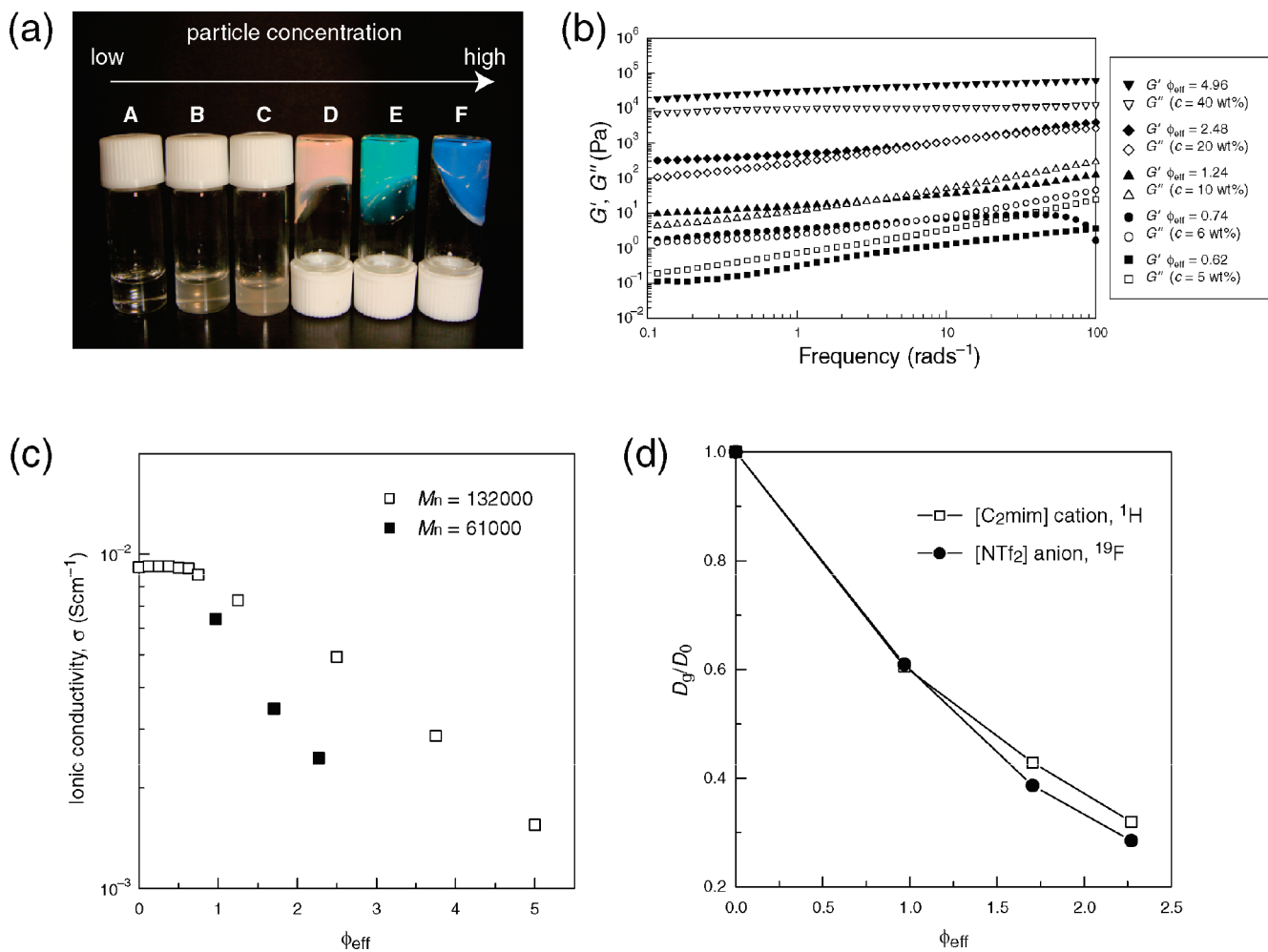


Figure 8. (a) Color photographs of colloidal suspensions of PMMA-g-NPs ($M_n = 91\,000$ g/mol for grafting PMMA, silica core radius = 61 nm) in $[\text{C}_2\text{mim}][\text{NTf}_2]$ with different particle concentrations. Mass concentration of PMMA-g-NPs (in wt %): A = $([\text{C}_2\text{mim}][\text{NTf}_2]) = 0$, B = 1.0, C = 3.0, D = 14.2, E = 25.0, and F = 33.3. (b) Elastic (G') and loss (G'') moduli as functions of frequency for suspensions of PMMA-g-NPs ($M_n = 132\,000$ g/mol for grafting PMMA, silica core radius = 61 nm) in an IL at 25 °C with different silica particle concentrations. (c) Ionic conductivity (σ) of suspensions of PMMA-g-NPs in $[\text{C}_2\text{mim}][\text{NTf}_2]$ at 25 °C as a function of particle concentration. (d) Relative diffusivity (D_g/D_0) of $[\text{C}_2\text{mim}]$ cations and $[\text{NTf}_2]$ anions in the colloidal glass consisting of PMMA-g-NPs ($M_n = 91\,000$ g/mol for grafting PMMA, silica core radius = 61 nm) with different particle concentrations. Reproduced from ref 63.

decrease rapidly was consistent with the glass-transition volume fraction ϕ_g . Although the conductivity values were lower than those of the colloidal gels, the colloidal glass also displayed a sufficient conductivity higher than 10^{-3} S cm⁻¹ at room temperature, even when it was in a highly concentrated glassy state. It should be noted that the macroscopic motion of PMMA-g-NP is frozen in the colloidal glass. The grafted PMMA chains are swollen in the IL and are locally mobile,⁶⁵ and the ionic motion is decoupled from the segmental motion of the grafting PMMA.⁶⁶ This explains the high ionic conductivity of colloidal glass. The relative diffusivity (D_g/D_0) of the ions showed a trend that was opposite to that for the colloidal gels (Figure 8d), with the reduction in D_g/D_0 for the $[\text{NTf}_2]$ anion being greater than that for the $[\text{C}_2\text{mim}]$ cation. These findings indicate that $[\text{NTf}_2]$ anions preferentially interact with PMMA chains, which is consistent with the results observed in ion gels consisting of a PMMA network polymer and $[\text{C}_2\text{mim}][\text{NTf}_2]$.⁶⁵ Thus, the D_g/D_0 values of anions and cations were influenced by the interaction with colloidal particles in these soft materials; accordingly, the

appropriate design of the interaction between ions and particles would offer a new procedure for the production of selective ion-conducting solid electrolytes.

As shown in Figure 8a, the colloidal glass consisting of submicrometer-sized PMMA-g-NPs exhibits different colors depending on particle concentrations. It is well known that monodisperse particles can form 3D periodic structures of particles that are known as colloidal crystals. The periodic dielectric structures prevent the propagation of an electromagnetic wave in a certain range on the basis of Bragg diffraction. In other words, the colloidal crystal shows a photonic band gap (PBG) or structural color. Accordingly, such materials have attracted considerable attention owing to their potential for applications in sensors, displays, and PBG materials.⁶⁷ The colloidal glass did not contain any chromophores capable of absorbing visible light; therefore, the observed colors were a consequence of the structural color. Although our colloidal glassy materials were expected to have only a short-range-ordered amorphous structure, reflection spectra revealed that they had

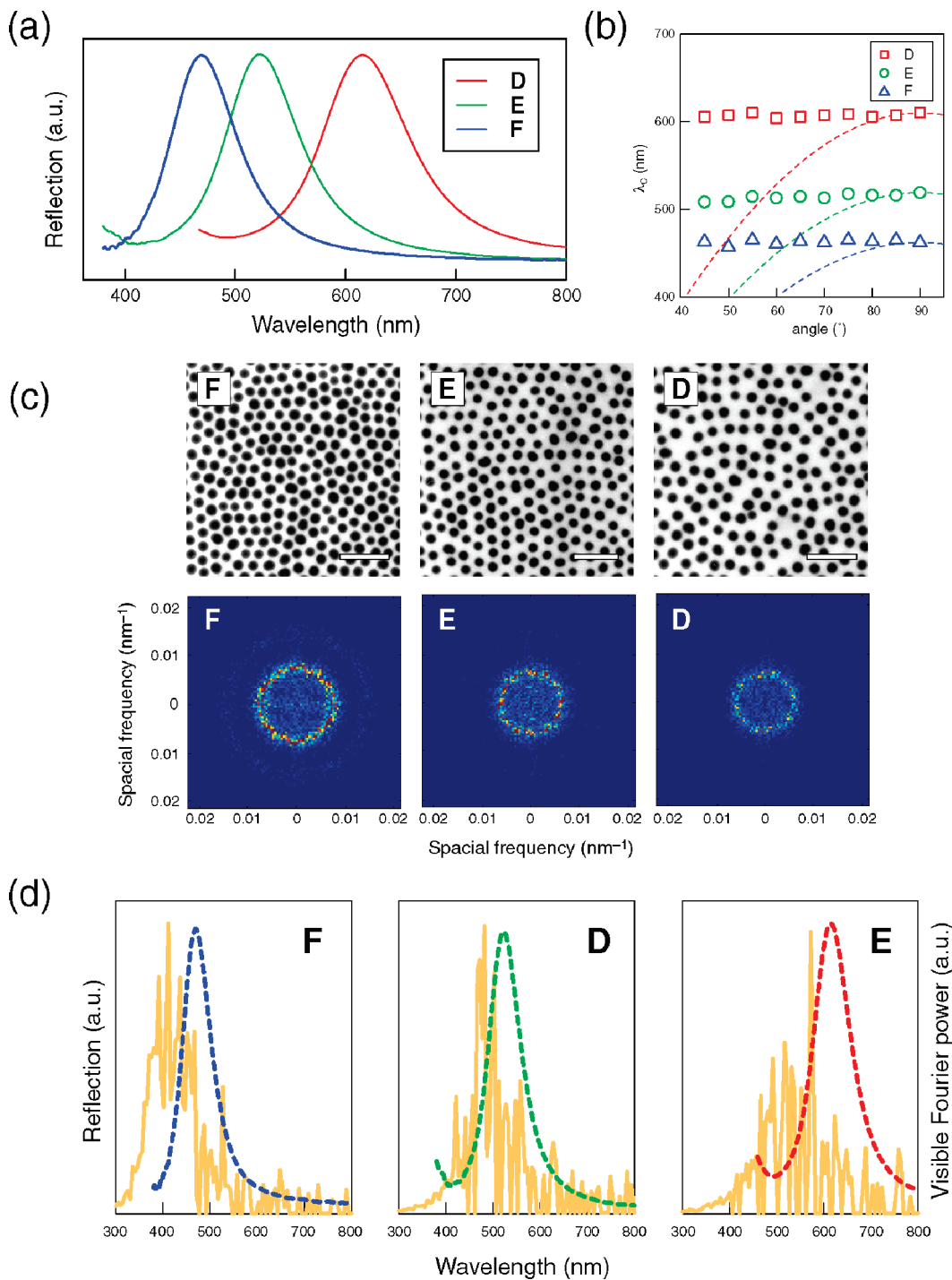


Figure 9. (a) Reflection spectra of colloidal glass. (b) Reflection peak measured as a function of the angle between the incident light and the supported glass substrate. The dashed lines show the behavior predicted by Bragg's law. (c) TEM images (top) and corresponding 2D Fourier power spectra (bottom). The scale bar is 500 nm. (d) Reflection spectra; the broken lines show the measured spectra whereas the solid lines show the spectra predicted from 2D Fourier power spectroscopy. Samples D–F correspond to the same samples shown in Figure 8a. Reproduced from ref 62.

structural colors corresponding to the observed colors (Figure 9a). Furthermore, the structural colors could be tuned from red to blue by adjusting the particle concentrations. Notable differences in the structural color between typical colloidal crystals and our colloidal glass were also confirmed on the basis of their angle dependence. The colloidal glass showed homogeneous, nonbrilliant, angle-independent structural color, whereas the

intense diffraction of typical colloidal crystals obeyed angle-dependent Bragg's law (Figure 9b). This unique optical property of the colloidal glass was further investigated with respect to the microstructure. Figure 9c shows TEM images of the colloidal glasses and their 2D Fourier power spectra. As shown in the TEM images, spatial periodicity without long-range order is strong evidence that the colloidal glasses are actually amorphous.

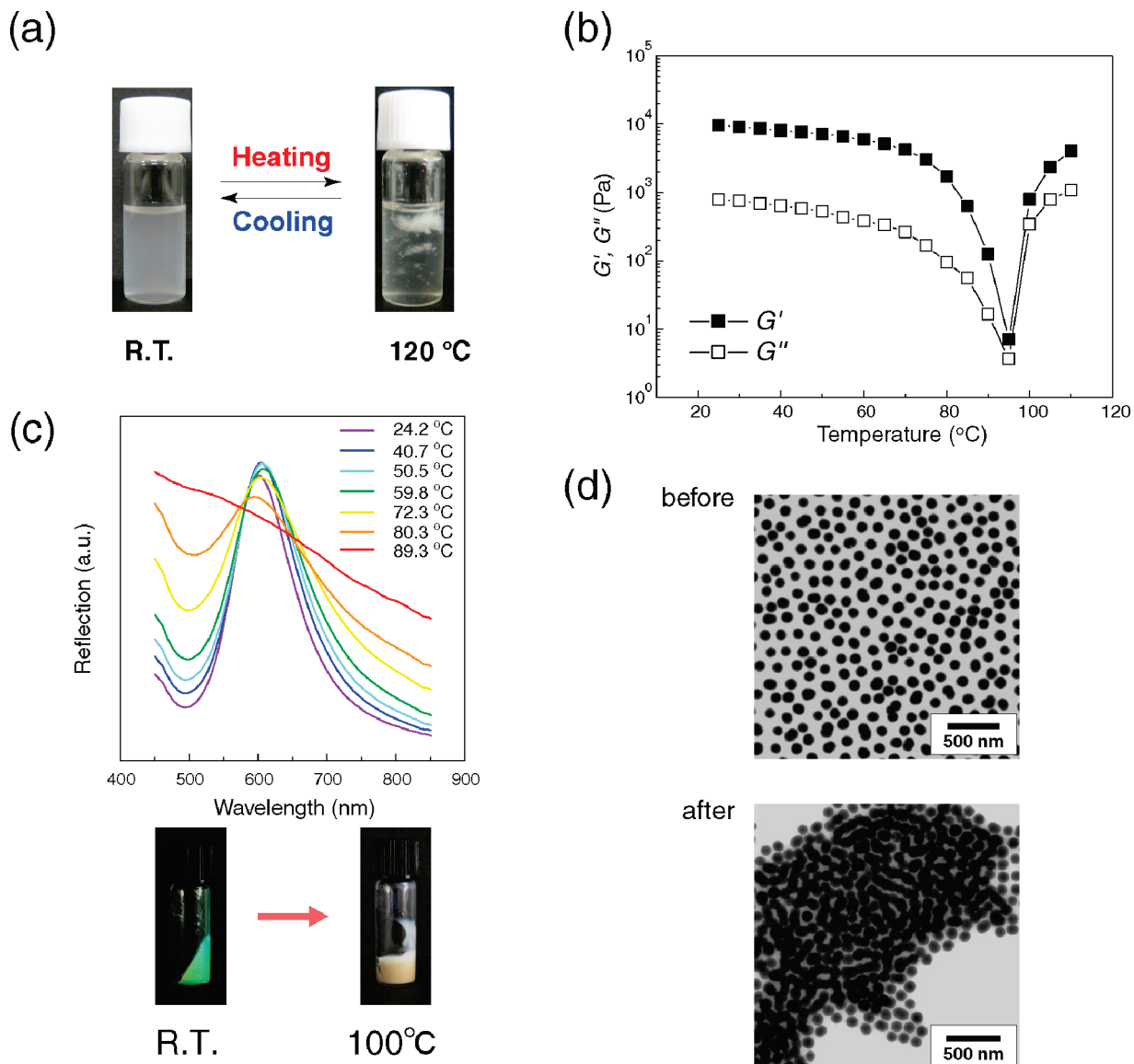


Figure 10. (a) Optical images of 1 wt % PBnMA-g-NP suspension in $[C_2mim][NTf_2]$ at room temperature (left) and 120 °C (right). (b) Temperature dependence of storage modulus G' (solid symbols) and loss modulus G'' (open symbols) for 25.0 wt % PBnMA-based colloidal glass in $[C_2mim][NTf_2]$. (c) Reflection spectra of 25 wt % PBnMA-based colloidal glass at different temperatures. Structural color changes before and after heating to 100 °C. (d) TEM images of 25.0 wt % PBnMA-based colloidal glass before and after heating to 100 °C. Reproduced from ref 69.

The ring-shaped 2D Fourier power spectra indicate that the colloidal glasses are equivalently nanostructured in all directions, which explains the angle-independent optical properties. We predicted the reflection spectra from the 2D Fourier power spectra using a method similar to that adopted for the evaluation of structural color found in the colored epidermis of certain animals and insects by Prum et al.⁶⁸ Figure 9d shows the reflection spectra predicted from the radial averages of the 2D Fourier power spectra and the average refractive indices of the colloidal glasses in the IL. For comparison, experimentally measured reflection spectra are also shown by the broken lines. Although the reflection peaks in the predicted spectra were located at slightly blue-shifted wavelengths as compared to those in the measured reflection spectra, the peaks in both spectra coincided reasonably well with the wavelengths of the observed colors. Relatively good agreement of the measured reflection spectra under the 3D condition with

the predicted reflection spectra obtained from 2D Fourier power spectral analysis suggests that the particle arrangement observed in the TEM images is representative of the short-range-ordered structure of the colloidal glass.

3-3. Colloidal Glass-to-Colloidal Gel Transition. Here, we demonstrate the colloidal glass-to-gel transition with thermosensitive polymer-grafted silica nanoparticles.⁶⁹ In a previous study, we reported that poly(benzyl methacrylate) (PBnMA) linear polymer discretely exhibited a lower critical solution temperature (LCST) phase separation in ILs at the phase-separation temperature (T_c). Specifically, PBnMA was found to be soluble at lower temperatures but insoluble at temperatures higher than T_c .⁷⁰ When PBnMA-g-NPs were used instead of PMMA-g-NPs, the colloidal stability of PBnMA-g-NPs in $[C_2mim][NTf_2]$ was expected to change from a sterically suspended state to an aggregated state in response to increased temperature. As expected, the aggregation

of PBnMA-g-NPs in a dilute suspension was observed after heating to above the T_c (Figure 10a). Moreover, the highly concentrated colloidal glass of PBnMA-g-NPs exhibited an interesting change in the rheological and optical properties in response to temperature. As shown in Figure 10b, a V-shaped rheological response was observed upon heating. Specifically, both G' and G'' first decreased with increasing temperature to 95 °C, above which they increased. In terms of the optical properties, the colloidal glass exhibited a clear structural color at room temperature. The baselines of the reflection peaks increased significantly, and the peak intensity weakened upon heating (Figure 10c). The reflection peak was no longer detected at 89.3 °C, and the sample became opaque at 100 °C. As a result of the desolvation of the grafted PBnMA at higher temperatures, interparticle attraction arising from the disappearance of the steric effect and the phase separation of PBnMA caused particle flocculation, leading to the interconnection of the particulate network. Such formation of colloidal gels resulted in an increase in the moduli at higher temperature, whereas the first decrease in the moduli was governed by the reduction in the particle volume fraction of the colloidal glass that occurred in response to the deswelling of the grafted PBnMA. Simultaneously, the short-range-ordered structure of the colloidal glass was transformed into a completely disordered structure at higher temperatures. The incoherent scattering derived from aggregated PBnMA-g-NPs was responsible for the optical properties of the heated sample, where most of the incident light was randomly scattered. These findings indicate that the temperature-induced V-shaped viscoelastic behavior and the change in the structural color of the PBnMA-based colloidal glass were the result of a colloidal glass-to-gel transition. Figure 10d shows TEM images of PBnMA-based colloidal glass before and after heating to 120 °C. Most of the silica core particles before heating were separated from each other by the grafted PBnMA chains, and the particles adhered to each other and formed large aggregates after heating. These observations also demonstrate the colloidal glass-to-gel transition of the PBnMA-based colloidal glass in $[C_2mim][NTf_2]$.

4. CONCLUDING REMARKS

We evaluated the colloidal stability in ILs by focusing on three different repulsive interactions between colloidal particles—electrostatic, steric, and solvation forces in the absence and presence of stabilizers. Although the unique properties of ILs, which can enable applications of ILs to colloid systems, are primarily dominated by their ionic nature, the high ionic atmosphere makes the electrostatic repulsion inefficient owing to charge screening in the ILs. Alternatively, the steric and solvation forces effectively stabilize colloidal particles in ILs. Accordingly, it has been proposed that IL-based steric forces and IL-based solvation forces account for the experimental evidence of unusual colloidal stabilization in ILs without any stabilizers. We emphasize that these stabilizer-free colloidal stabilization mechanisms should be more pronounced in ILs than in typical molecular solvents. One of the most fascinating properties, the structure-forming property of ILs, can promote the encapsulation of colloidal particles in ILs, leading to the IL-based steric force. The property of bulk structure formation combined with the ionic characteristics can also contribute to the formation of the well-defined layered structure on the charged colloidal surface (i.e., IL-based solvation force). Furthermore, the properties of ILs can be tuned by selecting cations and anions. The

numerous varieties of combinations of available ions allow the optimization of ILs that is suitable for stabilizing colloidal particles in the ILs.

On the basis of the findings presented above, we generated two different functional soft materials formed by the self-assembly of colloidal particles in ILs. Colloidal gels were prepared using unstable silica colloidal particles that formed an aggregated network in ILs, and colloidal glasses were formed by highly concentrated suspensions of sterically stabilized polymer-grafted silica particles above the colloidal glass-transition volume fraction. The colloidal approach to obtaining soft solids based on ILs utilizing the colloidal gel and the colloidal glass offers an interesting path toward the preparation of IL-based solid electrolytes with sufficiently high conductivity. The shear-induced fluidic properties of these materials may become an advantage in terms of facile processability.

Owing to their phase-separated nature, colloidal gels containing a small number of silica nanoparticles formed interconnected network structures, resulting in the gels showing liquidlike high ionic conductivity despite the solidlike rheological response. In addition, two distinct rheological responses were observed in the suspensions of hydrophilic fumed silica in different ILs—colloidal gelation and shear thinning in flocculated systems and shear thickening in stable suspensions.

The colloidal glass exhibited homogeneous, nonbrilliant, angle-independent structural colors. The colors could be tuned to cover the entire visible wavelength spectrum by changing the particle concentrations. Although the structural color of the short-range-ordered structure was not as intense as that of conventional colloidal crystals with long-range order, the isotropic optical properties would make them useful for the development of selectively light-reflective materials for optical devices with wide viewing angles. The colloidal glass with high ionic conductivity and unique photonic properties may be of interest for use in devices in which photons and/or ions play a crucial role.

To design colloidal soft materials with ILs, other functionalities can be introduced into each component. As an example, we prepared a colloidal glass of PBnMA-grafted silica nanoparticles in which the PBnMA chain showed LCST behavior in $[C_2mim][NTf_2]$. The thermosensitive colloidal glass presented a V-shaped rheological response and a structural color change in response to the colloidal glass-to-gel transition. This basic principle is expected to be applicable to suspensions of many other functional colloidal particles such as metals, semiconductors, and magnetic particles in ILs. Such a significant flexibility in material design opens infinite possibilities for the fabrication of advanced materials with multifunctional properties.

■ AUTHOR INFORMATION

Corresponding Author

*Tel/Fax: +81-45-339-3955. E-mail: mwatanab@ynu.ac.jp.

■ ACKNOWLEDGMENT

We gratefully acknowledge the financial support of a grant-in-aid for scientific research from the MEXT, Japan (no. 452-17073009 and no. B-20350104).

■ REFERENCES

- (1) Welton, T. *Chem. Rev.* **1999**, *99*, 2071.

- (2) Fei, Z.; Geldbach, T. J.; Zhao, D.; Dyson, P. J. *Chem.—Eur. J.* **2006**, *12*, 2122.
- (3) Zakeeruddin, S. M.; Grätzel, M. *Adv. Mater.* **2009**, *19*, 2187.
- (4) Lewandowski, A.; Świderska-Mocek, A. *J. Power Sources* **2009**, *194*, 601.
- (5) Lee, S.-Y.; Ogawa, A.; Kanno, H.; Nakamoto, H.; Yasuda, M.; Watanabe, M. *J. Am. Chem. Soc.* **2010**, *132*, 9764.
- (6) Ueno, K.; Tokuda, H.; Watanabe, M. *Phys. Chem. Chem. Phys.* **2010**, *12*, 1649.
- (7) Earle, M. J.; Esperança, J. M. S. S.; Gilea, M. A.; Lopes, J. N. C.; Rebello, L. P. N.; Magee, J. W.; Seddon, K. R.; Widgren, J. A. *Nature* **2006**, *439*, 831.
- (8) Lopes, J. N. A. C.; Pádua, A. A. H. *J. Phys. Chem. B* **2006**, *110*, 3330.
- (9) Triolo, A.; Russina, O.; Bleif, H.-J.; Cola, E. D. *J. Phys. Chem. B* **2007**, *111*, 4641.
- (10) Anderson, J. L.; Pino, V.; hagberg, E. C.; Sheares, V. V.; Armstrong, D. W. *Chem. Commun.* **2003**, 2444.
- (11) Fletcher, K. A.; Pandey, S. *Langmuir* **2004**, *20*, 33.
- (12) He, Y.; Li, Z.; Simone, P.; Lodge, T. P. *J. Am. Chem. Soc.* **2006**, *128*, 2745.
- (13) Binks, B. P.; Dyab, A. K. F.; Fletcher, P. D. I. *Chem. Commun.* **2003**, 2540.
- (14) Gao, H.; Li, J.; Han, B.; Chen, W.; Zhang, J.; Zhang, R.; Yan, D. *Phys. Chem. Chem. Phys.* **2004**, *6*, 2914.
- (15) Fonseca, G. S.; Machado, G.; Teixeira, S. R.; Fecher, G. H.; Morais, J.; Alves, M. C. M.; Dupont, J. *J. Colloid Interface Sci.* **2006**, *301*, 193.
- (16) Zhao, D.; Fei, Z.; Ang, W. H.; Dyson, P. J. *Small* **2006**, *2*, 879.
- (17) Gelesky, M. A.; Umpierre, A. P.; Machado, G.; Correia, R. R. B.; Magno, W. C.; Morais, J.; Ebeling, G.; Dupont, J. *J. Am. Chem. Soc.* **2005**, *127*, 4588.
- (18) Jacob, D. S.; Genish, I.; Klein, L.; Gedanken, A. *J. Phys. Chem. B* **2006**, *110*, 17711.
- (19) Endres, F. *ChemPhysChem* **2002**, *3*, 144.
- (20) Torimoto, T.; Okazaki, K.; Kiyama, T.; Hirahara, K.; Tanaka, N.; Kuwabata, S. *Appl. Phys. Lett.* **2006**, *89*, 243117.
- (21) Dupont, J.; Fonseca, G. S.; Umpierre, A. P.; Fichtner, P. F. P.; Teixeira, S. R. *J. Am. Chem. Soc.* **2002**, *124*, 4228.
- (22) Wojtków, W.; Trzeciak, A. M.; Choukroun, R.; Pellegatta, J. L. *J. Mol. Catal. A: Chem.* **2004**, *224*, 81.
- (23) Zhou, Y.; Antonietti, M. *J. Am. Chem. Soc.* **2003**, *125*, 14960.
- (24) Ma, Z.; Yu, J.; Dai, S. *Adv. Mater.* **2010**, *22*, 261.
- (25) Olivier-Bourbigou, H.; Magna, H. L.; Morvan, D. *Appl. Catal., A* **2010**, *373*, 1.
- (26) Torimoto, T.; Tsuda, T.; Okazaki, K.; Kuwabata, S. *Adv. Mater.* **2010**, *22*, 1196.
- (27) Itoh, H.; Naka, K.; Chujo, Y. *J. Am. Chem. Soc.* **2004**, *126*, 3026.
- (28) Wei, G.-T.; Yang, Z.; Lee, C.-Y.; Yang, H.-Y.; Wang, C. R. C. *J. Am. Chem. Soc.* **2004**, *126*, 5036.
- (29) Migowski, P.; Dupont, J. *Chem.—Eur. J.* **2006**, *13*, 32.
- (30) Gu, Y.; Li, G. *Adv. Synth. Catal.* **2009**, *351*, 817.
- (31) Fukushima, T.; Kosaka, A.; Ishimura, Y.; Yamamoto, T.; Takigawa, T.; Ishii, N.; Aida, T. *Science* **2003**, *300*, 2072.
- (32) Nakashima, T.; Kawai, T. *Chem. Commun.* **2005**, 1643.
- (33) Guerrero-Sánchez, C.; Lara-Ceniceros, T.; Jimenez-Regalado, E.; Raşa, M.; Schubert, U. S. *Adv. Mater.* **2007**, *19*, 1740.
- (34) Wang, P.; Zakeeruddin, S. M.; Comte, P.; Exnar, I.; Grätzel, M. *J. Am. Chem. Soc.* **2003**, *125*, 1166.
- (35) Sun, J.; Bayley, P.; MacFarlane, D. R.; Forsyth, M. *Electrochim. Acta* **2007**, *52*, 7083.
- (36) Simano, S.; Zhou, H.; Honma, I. *Chem. Mater.* **2007**, *19*, 5216.
- (37) Israelachvili, J. *Intermolecular and Surface Forces*, 2nd ed.; Academic Press: San Diego, 1991.
- (38) Ueno, K.; Inaba, A.; Kondoh, M.; Watanabe, M. *Langmuir* **2008**, *24*, 5253.
- (39) Kornyshev, A. A. *J. Phys. Chem. B* **2007**, *111*, 5545.
- (40) Fitchett, B. D.; Conboy, J. C. *J. Phys. Chem. B* **2004**, *108*, 20255.
- (41) Pinilla, C.; Del popolo, M. G.; Lynden-Bell, R. M.; Kohanoff, J. *J. Phys. Chem. B* **2005**, *109*, 17922.
- (42) Sha, M.; Wu, G.; Dou, Q.; Tang, Z.; Fang, H. *Langmuir* **2010**, *26*, 12667.
- (43) Horn, R. G.; Israelachvili, J. N. *J. Chem. Phys.* **1981**, *75*, 1400.
- (44) Mizukami, M.; Kusakabe, K.; Kurihara, K. *Prog. Colloid Polym. Sci.* **2004**, *128*, 105.
- (45) Israelachvili, J.; Wennerström, H. *Nature* **1996**, *379*, 218.
- (46) Atkin, R.; Warr, G. G. *J. Phys. Chem. C* **2007**, *111*, 5162.
- (47) Horn, R. G.; Evans, D. F.; Ninham, B. W. *J. Phys. Chem.* **1988**, *92*, 3538.
- (48) Min, Y.; Akbulut, M.; Sangoro, J. R.; Kremer, F.; Prud'homme, R. K.; Israelachvili, J. *J. Phys. Chem. C* **2009**, *113*, 16445.
- (49) Perkin, S.; Albrecht, T.; Klein, J. *Phys. Chem. Chem. Phys.* **2010**, *12*, 1243.
- (50) Hayes, R.; Warr, G. G.; Atkin, R. *Phys. Chem. Chem. Phys.* **2010**, *12*, 1709.
- (51) Ueno, K.; Kasuya, M.; Watanabe, M.; Mizukami, M.; Kurihara, K. *Phys. Chem. Chem. Phys.* **2010**, *12*, 4066.
- (52) Mezger, M.; Schröder, H.; Reichert, H.; Schramm, S.; Okasinski, J. S.; Schröder, S.; Honkimäki, V.; Deutsch, M.; Ocko, B. M.; Ralston, J.; Rohwerder, M.; Stratmann, M.; Dosch, H. *Science* **2008**, *322*, 424.
- (53) Ott, L. S.; Cline, M. L.; Deetlefs, M.; Seddon, K. R.; Finke, R. G. *J. Am. Chem. Soc.* **2005**, *127*, 5758.
- (54) Campbell, P. S.; Santini, C. C.; Bouchu, D.; Fenet, B.; Philippot, K.; Chaudret, B.; Pádua, A. A. H.; Chauvin, Y. *Phys. Chem. Chem. Phys.* **2010**, *12*, 4217.
- (55) Ren, L.; Meng, L.; Lu, Q.; Fei, Z.; Dyson, P. J. *J. Colloid Interface Sci.* **2008**, *323*, 260.
- (56) Smith, J.; Werzer, O.; Webber, G. B.; Warr, G. G.; Atkin, R. *J. Phys. Chem. Lett.* **2010**, *1*, 64.
- (57) Ueno, K.; Imaizumi, S.; Hata, K.; Watanabe, M. *Langmuir* **2009**, *25*, 825.
- (58) Stokes, J. R.; Frith, W. *J. Soft Matter* **2008**, *4*, 1133.
- (59) Ueno, K.; Hata, K.; Katakabe, T.; Kondoh, M.; Watanabe, M. *J. Phys. Chem. B* **2008**, *112*, 9013.
- (60) Allain, C.; Cloitre, M.; Wafra, M. *Phys. Rev. Lett.* **1995**, *74*, 1478.
- (61) Romero, C. R.; Baldelli, S. *J. Phys. Chem. B* **2006**, *110*, 6213.
- (62) Ueno, K.; Inaba, A.; Sano, Y.; Kondoh, M.; Watanabe, M. *Chem. Commun.* **2009**, 3603.
- (63) Ueno, K.; Sano, Y.; Inaba, A.; Kondoh, M.; Watanabe, M. *J. Phys. Chem. B* **2010**, *114*, 13095.
- (64) van Megen, W.; Mortensen, T. C.; Williams, S. R.; Müller, J. *Phys. Rev. E* **1998**, *58*, 6073.
- (65) Susan, M. A. B. H.; Kaneko, T.; Noda, A.; Watanabe, M. *J. Am. Chem. Soc.* **2005**, *127*, 4976.
- (66) Seki, S.; Susan, M. A. H. S.; Kaneko, T.; Tokuda, H.; Noda, A.; Watanabe, M. *J. Phys. Chem. B* **2005**, *109*, 3886.
- (67) Takeoka, Y.; Watanabe, M. *Adv. Mater.* **2003**, *15*, 199.
- (68) Prum, R. O.; Torres, R. H. *J. Exp. Biol.* **2003**, *206*, 2409.
- (69) Ueno, K.; Inaba, A.; Ueki, T.; Kondoh, M.; Watanabe, M. *Langmuir* **2010**, *26*, 18031.
- (70) Ueki, T.; Watanabe, M. *Langmuir* **2007**, *23*, 988.